

Intensity Distribution of Modes in Surface Corrugated Waveguides

A. García-Martín, J.A. Torres, J.J. Sáenz

Departamento de Física de la Materia Condensada and Instituto de Ciencia de Materiales “Nicolás Cabrera”, Universidad Autónoma de Madrid, E-28049 Madrid, Spain.

M. Nieto-Vesperinas

Instituto de Ciencia de Materiales de Madrid. Consejo Superior de Investigaciones Científicas, Campus de Cantoblanco, E-28049 Madrid, Spain.
(11 November 1997)

Phys. Rev. Lett. 80, 4165 (1998)

©1998 The American Physical Society

Exact calculations of transmission and reflection coefficients in surface randomly corrugated optical waveguides are presented. As the length of the corrugated part of the waveguide increases, there is a strong preference to forward coupling through the lowest mode. An oscillating behavior of the enhanced backscattering as a function of the wavelength is predicted. Although the transport is strongly non isotropic, the analysis of the probability distributions of the transmitted waves confirms in this configuration distributions predicted by Random Matrix Theory for volume disorder.

PACS numbers: 42.25.Bs, 05.60.+w, 41.20.Jb, 84.40.Az

Defects and inhomogeneities in waveguides are a subject of increasing research for its influence on the propagation of both classical and quantum waves [1]. Volume defects have recently been studied in connection with the propagation of electrons through two-dimensional (2D) wires [2–4]. On the other hand, slight surface roughness has been considered both in electron transport through thin films [5] as well as in optical fibers and waveguides [6], mainly in connection with attenuation. Recently, some analogies between electron transport and propagation of diffuse light through surface corrugated waveguides have been put forward [7]. However, the assumption of diffuse incoming waves limits the study to those systems in which the incident modes are mutually incoherent.

In this letter we address the more practical situation in light propagation where a single incident mode couples with different forward and backward modes [8]. As we shall see, the scattering from rough, perfectly conducting, walls (see Fig.1) induces a strong and rich coupling to forward and backward modes. The coupling characteristics present significant differences with respect to the coupling induced by volume defects. For any incoming mode, and when the length of the system is larger than the localization length ξ , there is a strong preference for the forward propagation through the lowest mode. The coupling to backward modes presents a very interesting behavior, depending on the incident mode. The “external” modes (defined as those propagating modes with either the smallest or the largest transversal momentum) present enhanced backscattering factor larger than the

others. In the case of the lowest mode, this factor exhibits remarkable oscillations as a function of the wavelength. We shall also present an extensive analysis of the statistical properties of the different transmission coefficients. As far as we know, this has been carried out only for the case of volume defects. In the diffusive regime, the theoretical predictions of Ref. [9] (and subsequently, Ref. [10]) have recently been confirmed experimentally [11]. A crossover from either the Rayleigh and Gaussian statistics in the diffusive regime to lognormal statistics in the localized regime, expected from numerical simulations [12], has been analytically deduced in Ref. [13]. Although the mode coupling is quite different in the case of surface roughness, our calculated distributions of transmittivities are fully consistent with the predicted behavior for bulk disordered waveguides.

The corrugated part of the waveguide, of total length L and perfectly reflecting walls, is composed of n slices of length l . The width of each slice has random values uniformly distributed between $W_0 - \delta$ and $W_0 + \delta$ about a mean value W_0 . We shall take $W_0/\delta = 7$ and $l/\delta = 3/2$. The main transport properties do not depend on the particular choice of these parameters, however. We consider s-polarized waves with the electric field parallel to the surface grooves (TE modes). Transmission and reflection coefficients are exactly calculated by solving the 2D wave equation by mode matching at each slice, together with a generalized scattering matrix technique [7,14,15].

For a given incoming mode i , the transmission (T_{ij}) and reflection (R_{ij}) coefficients are defined by

$$T_{ij} = \frac{\Phi_j^{Forw}}{\Phi_i^{in}}, \text{ and } R_{ij} = \frac{\Phi_j^{Back}}{\Phi_i^{in}}, \quad (1)$$

Φ_j^{Forw} being the total flux transmitted into the forward outgoing mode j , Φ_j^{Back} the total flux reflected into the backward outgoing mode j , and Φ_i^{in} the total flux of the incident mode. The total transmission for the incoming mode i , is given by $T_i = \sum_j T_{ij}$, and $G = \sum_i T_i$ is the normalized transmittance (conductance). Ensemble averages, denoted by $\langle \cdot \rangle$, are performed over a thousand realizations of the corrugated waveguide (unless otherwise stated).

The analysis of the *conductance* of surface corrugated waveguides is qualitatively similar to the electron transport in disordered nanowires. For short lengths the transport regime is diffusive with an effective mean free path [7] $\ell = (N\partial\langle 1/G \rangle / \partial L)^{-1}$, where N is the number of propagating modes. The transport regime changes as L becomes of the order of the localization length [16] $\xi = -(\partial\langle \ln(G) \rangle / \partial L)^{-1}$, with $\xi = N\ell$ within the numerical accuracy [7]. However, the analysis of the transmission coefficients T_{ij} reveals qualitative differences between random surface and volume scattering.

As a typical example, let us consider that the ratio between the waveguide width and the wavelength is $W_0/\lambda = 2.6$. This allows five propagating modes. In Fig. 1 we plot $\langle \ln(T_{ij}) \rangle$, as a function of the normalized length L/W_0 for two different incident modes $i = 1$ and $i = 3$ (Fig. 1 shows the average over 100 different realizations for each length L). All curves present the same linear dependence at large L . The inverse of the slope defines a length $\xi_{ij} = -(\partial\langle \ln(T_{ij}) \rangle / \partial L)^{-1}$ which *does not depend on the incoming or outgoing modes* ($\xi_{ij}/W_0 = 34.4 \pm 0.7$ for the structure calculated in Fig. 1). Exactly the same dependence is found for $\langle \ln T_i \rangle$. As a general result, and within the numerical accuracy, $\xi_{ij} = \xi_i = \xi = N\ell$.

In contrast with the expected isotropic mode distribution induced by scattering from volume defects, the calculation of T_{ij} and T_i shows a clear non isotropic distribution, even in the diffusive regime ($\ell \leq L \leq \xi$) as shown in Fig. 2(a-c). In the localized regime ($L > \xi$), for any incoming mode i there is a strong preference to couple with the lowest transmitted mode $j = 1$. The coupling to forward modes decreases as their transversal (longitudinal) momenta increase (decrease).

Concerning backward modes, Fig. 1 shows the averaged reflection coefficients $\langle R_{ij} \rangle$ as functions of the length L . Enhanced backscattering effects (EB) can be clearly seen in this figure. Coherent EB arising in the light scattering both from dense media [17] and rough surfaces [18] has been intensively investigated [1]. For a waveguide with N propagating modes, Random Matrix Theory (RMT) predicts [19,20] that the EB peak is 2 the scattering to any other channel, irrespective of the incoming mode. However, although not explicitly discussed, numerical calculations in waveguides with volume disorder

[4] show factors other than 2 for EB of “external” modes. In order to quantify the EB peak, we define, for a given incoming mode i , an *enhanced backscattering factor* η_i as,

$$\eta_i = (N - 1) \frac{\langle R_{ii} \rangle}{\left(\sum_{j \neq i} \langle R_{ij} \rangle \right)}. \quad (2)$$

Fig. 2d shows η_i versus L . While the “central” modes ($i = 2, 3, 4$) present a factor $\eta \approx 2$, the “external” ($i = 1, 5$) modes have a much larger enhanced backscattering factor (≈ 4). This qualitative behavior, which also confirms indications for electron propagation in disordered wires [4], depends on the wavelength. The backscattering factor for the lowest mode η_1 oscillates above $\eta \approx 2$ as the wavelength λ decreases (i.e. W_0/λ increases) having its maxima close to half integers of W_0/λ , which correspond to the appearance of a new propagating mode in the waveguide [21]. This behavior is highly correlated with the oscillations both in the mean free path ℓ and in the localization length ξ [7] (the maxima in η correspond to minima in ξ). Just after the appearance of a new mode the backscattering dominates at this new appearing channel. This gives a very large η factor at the onset of the new mode, which slowly decreases to $\eta = 2$ as λ decreases. By contrast, the “central” modes present an almost constant enhanced backscattering factor near 2.

Let us now discuss the intensity probability distributions of the transmitted waves. As shown above, the behavior of the different averaged transmitivities for a surface disordered waveguide is qualitatively different from that obtained for volume disordered wires. Therefore, the question now is: does surface disorder change the probability distributions from those expected in bulk disordered systems?. In the case of random wires, diagrammatic techniques combined with RMT [9,10] show that in the diffusive regime the speckle pattern probability density $P(T_{ij})$ follows a Rayleigh statistics with stretched exponential tails, while the distribution $P(T_i)$ is Gaussian with tail deviations. Nonperturbative calculations done in absence of time reversal symmetry predict that these distributions evolve into the same lognormal distribution as the length L increases beyond the localization length ξ as expected from the numerical simulations of Ref. [12].

Fig. 3a contains the distribution $P(T_i / \langle T_i \rangle)$ for different values of $\langle T_i \rangle$. Although for a fixed length, the distributions vary from mode to mode, we find that, as long as $L \leq \xi$, the distribution does not depend on the incoming mode i neither on the length L , but only depends on the averaged transmission coefficients. The inset in Fig. 3a shows $P(T_i / \langle T_i \rangle)$ for $i = 3, 4, 5$ all having the same average, $\langle T_i \rangle = 0.16$, but corresponding to different lengths of the disordered region (see Fig. 2c). For the same average, modes $i = 1, 2$ are localized and have

a different distribution (see below). The speckle distribution $P(T_{ij}/\langle T_{ij} \rangle)$, in the diffusive regime follows an almost perfect Rayleigh statistics $P(x) = \exp(-x)$ (see Fig. 3b). Clear deviations from this exponential distribution are observed for $L \leq \ell$ (not shown in the figure) and for $L \geq \xi$. An interesting point is that the dependence of $\langle T_{ij} \rangle$ with length does not fix, by itself, the transport regime. While for $\ell < L < \xi$ all coefficients follow Rayleigh statistics, their dependence with L change completely from one to another as can be observed in Fig. 2a,b.

Except for either small lengths $L \leq \ell$ or large transmittivities ($\langle T_i \rangle \geq 1/2$), the qualitative behavior of both $P(T_i/\langle T_i \rangle)$ and $P(T_{ij}/\langle T_{ij} \rangle)$ is basically the same as that obtained for disordered wires [9,10,13] (compare our Fig. 3 with Fig. 1 of reference [13]). Moreover, both distributions evolve into the same lognormal distribution as the length L increases beyond the localization length. This is shown in Fig. 4 where $P(\ln(\tau))$ is plotted versus $\ln(\tau)$, $\tau = T_i, T_{ij}$, for different values of $\langle \ln(\tau) \rangle$. Solid lines fitted there represent the lognormal distribution

$$P(x) = \left(\frac{1}{\pi 2 \sigma_x^2} \right)^{1/2} \exp \left[-\frac{(x - \langle x \rangle)^2}{2 \sigma_x^2} \right] \quad (3)$$

with $x = \ln(T_i), \ln(T_{ij})$. and $\text{var}(x) = \sigma_x^2 = (3/2)|\langle x \rangle|$. In the strong localization limit ($L \gg \xi$), where $|\langle \ln(\tau) \rangle| \approx L/\xi = L/(N\ell)$, we obtain $\sigma_x^2 \approx (3/2)L/\xi$. Nevertheless, although the dependence is the same as expected from RMT [13], the variance of the calculated distribution is 3/2 the mean in contrast with the expected value of twice the mean (cf. (11) of reference [13]). However, the analysis of the conductance G in the localized regime shows a lognormal distribution with a mean which is half the variance, in perfect agreement with RMT predictions [22,20]. This is shown in the inset of Fig. 4. The solid lines show the corresponding lognormal distribution (eq. 3 with $x = \ln(G)$) with $\text{var}(x) = \sigma_x^2 = 2|\langle x \rangle|$.

In conclusion, we have analyzed the coupling to forward and backward modes in surface corrugated waveguides. The coupling with backward modes yields enhanced backscattering peaks, which can be larger than those theoretically predicted for the case of the lowest and highest incident modes. We have shown important differences in the transport coefficients with respect to the case of volume scattering. However, the probability distributions are the same as those obtained for bulk disordered waveguides and wires. In particular we have found a crossover from Rayleigh and Gaussian distributions in the diffusive regime to the same lognormal distribution in the localized regime in good agreement with the predictions of Random Matrix Theory.

We would like to thank E. Bascones, A.J. Caamaño, G. Gómez-Santos and T. López-Ciudad for stimulating discussions. This work has been supported by the Dirección General de Investigación Científica y Técnica

(DGICYT) through Grant No. PB95-0061 and the European Union. A. G.-M. acknowledges partial financial support from the postgraduate grant program of the Universidad Autónoma de Madrid.

-
- [1] P. Sheng "Introduction to Wave Scattering, Localization and Mesoscopic Phenomena", Academic Press, N.Y. (1995); C.W.J Beenakker and H. van Houten, in *Solid State Physics: Advances in Research and Applications*, H. Ehrenreich and D. Turnbull (Academic, San Diego, 1991), Vol. 44; M. Nieto-Vesperinas and J.C. Dainty eds., "Scattering in Volumes and Surfaces", (North Holland, Amsterdam, 1990)
 - [2] H. Tamura and T. Ando, Phys. Rev. B **44**, 1792 (1991); T. Ando and H. Tamura, Phys. Rev. B **46**, 2332 (1992); K. Nikolić and A. MacKinnon, Phys. Rev. B **47**, 6555 (1993); T.N. Todorov, Phys. Rev. B **54**, 5801 (1996).
 - [3] Th.M. Nieuwenhuizen, Europhys. Lett. **24**, 269 (1993); A. Mosk, Th.M. Nieuwenhuizen and C. Barnes, Phys. Rev. B **53**, 15914 (1996); Th. M. Nieuwenhuizen and J.M. Luck, Phys. Rev. E **48**, 569 (1993).
 - [4] P. García-Mochales, P.A. Serena, N. García and J.L. Costa-Krämer, Phys. Rev. B **53**, 10 268 (1996); P. García-Mochales and P.A. Serena, Phys. Rev. Lett **79**, 2316 (1997).
 - [5] A.R. McGurn and A.A. Maradudin, Phys. Rev. B **30**, 3136 (1984); Z. Tešanović and M. V. Jarić, Phys. Rev. Lett. **57**, 2760 (1986).
 - [6] D. Marcuse, Bell Syst. Tech. J., **48**, 3233 (1969); D. Marcuse, "Theory of Dielectric Optical Waveguides", Academic Press, N.Y. 1974; D.G. Hall, Opt. Lett. **6**, 601 (1981).
 - [7] A. García-Martín, J.A. Torres, J.J. Sáenz and M. Nieto-Vesperinas, Appl. Phys. Lett, **71**, 1912 (1997).
 - [8] F. Ladouceur and L. Polodian, Opt. Lett. **21**, 1833 (1996).
 - [9] Th. M. Nieuwenhuizen and M.C.W. van Rossum, Phys. Rev. Lett. **74**, 2674 (1995).
 - [10] E. Kogan and M. Kaveh, Phys. Rev. B **52**, R3813 (1995)
 - [11] M. Stoytchev and A.Z. Genack, Phys. Rev. Lett. **79**, 309 (1997).
 - [12] I. Edrei, M. Kaveh and B. Shapiro, Phys. Rev. Lett. **62**, 2120 (1989)
 - [13] S.A. van Lagen, P.W. Brouwer and C.W.J. Beenakker, Phys. Rev. E **53**, R1344 (1996).
 - [14] A. Weisshaar, J. Lary, S. M. Goodnick and V.K. Tripathi. J. Appl. Phys. **70**, 355 (1991)
 - [15] J.A. Torres and J.J. Sáenz, Phys. Rev. Lett. **77** 2245 (1996); (unpublished).
 - [16] P.W. Anderson, D.J. Thouless, E. Abrahams and D.S. Fisher, Phys. Rev. B **22**, 3519 (1980). P.W. Anderson, Phys. Rev. B **23**, 4828 (1981); P.A. Lee, A.D. Stone and H. Fukuyama. Phys Rev. B **35**, 1039 (1987).
 - [17] Y. Kuga and J. Ishimaru, J. Opt. Soc. Am. A, **1**, 831 (1984); M.P. van Albada and A. Lagendijk, Phys. Rev.

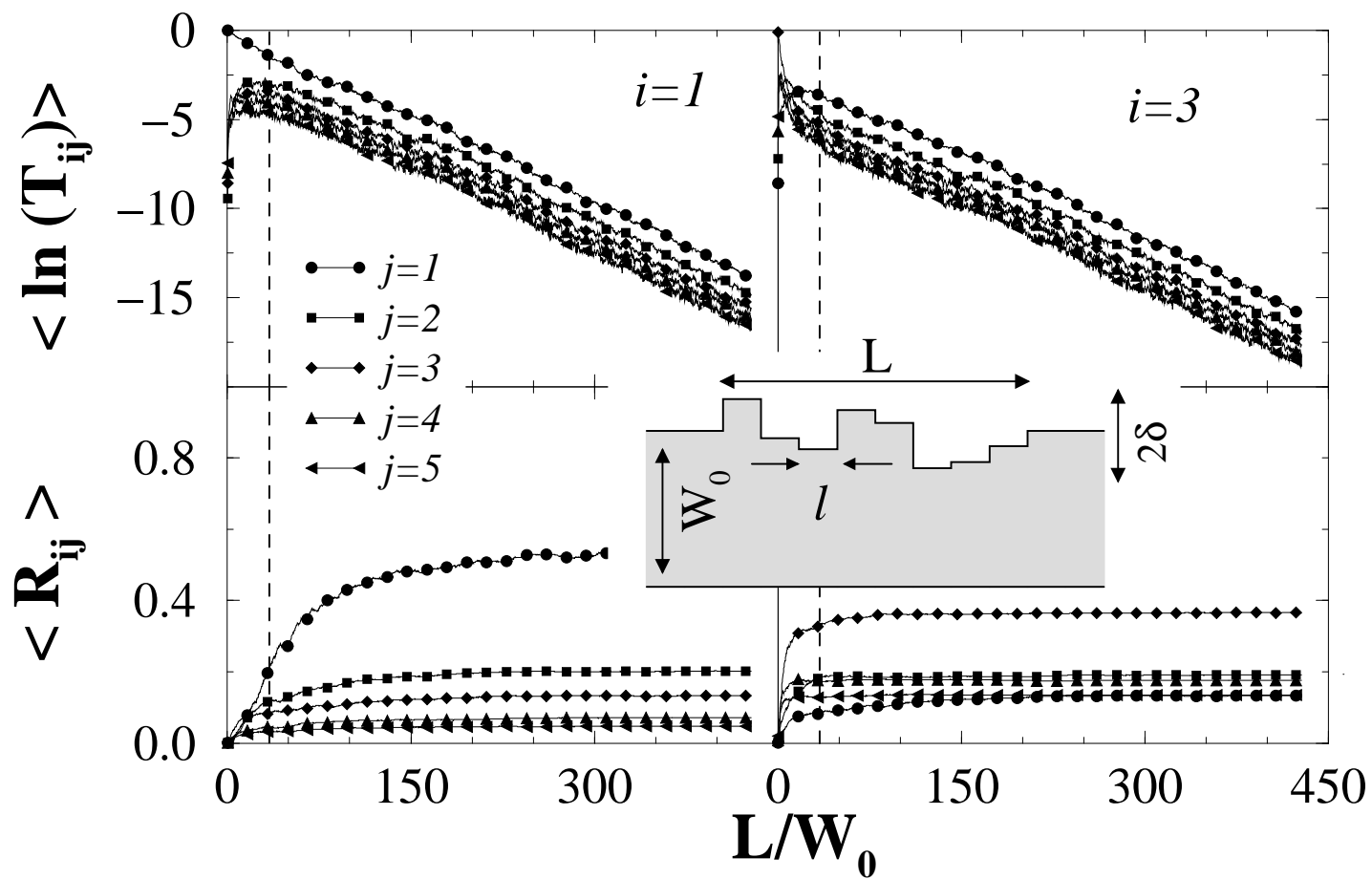
- Lett. **55**, 2692 (1985); P.E. Wolf and G. Maret, Phys. Rev. Lett. **55**, 1696 (1985); E. Akkermans, P.E. Wolf and R. Maynard, Phys. Rev. Lett. **56**, 1471 (1986); M. Kaveh, M. Rosenbuth, M. Edrei and I. Freud, Phys. Rev. Lett. **57**, 2949 (1986).
- [18] A.R. McGurn, A. Maradudin and V. Celli, Phys. Rev. B **31**, 4866 (1985); K.A. O'Donnell and E.R. Mendez, J. Opt. Soc. Am. A **4**, 1194 (1987); M. Nieto-Vesperinas and J.M. Soto-Crespo, Opt. Lett. **12**, 979 (1987).
- [19] P.A. Mello, E. Akkermans and B. Shapiro, Phys. Rev. Lett. **61**, 459 (1988); E. Bascones, M.J. Calderón, D. Castello, T. López and J.J. Sáenz, Phys. Rev. B **55**, R11911 (1997).
- [20] For a review see C.W.J. Beenakker, Rev. Mod. Phys. **69**, 731 (1997).
- [21] A. García-Martín *et al.*, unpublished.
- [22] Y. Imry, Europhys. Lett. **1**, 249 (1986); J.-L. Pichard, in *Quantum Coherence in Mesoscopic Systems*, ed. by B. Kramer, NATO-ASI Series **254**, 369 (Plenum, N.Y.) (1991).

FIG. 1. Averaged transmission (T_{ij}) and reflection (R_{ij}) coefficients (incoming mode i ; outgoing mode j) as a function of the normalized length of the disordered region L/W_0 . Inset: Schematic view of the system under consideration.

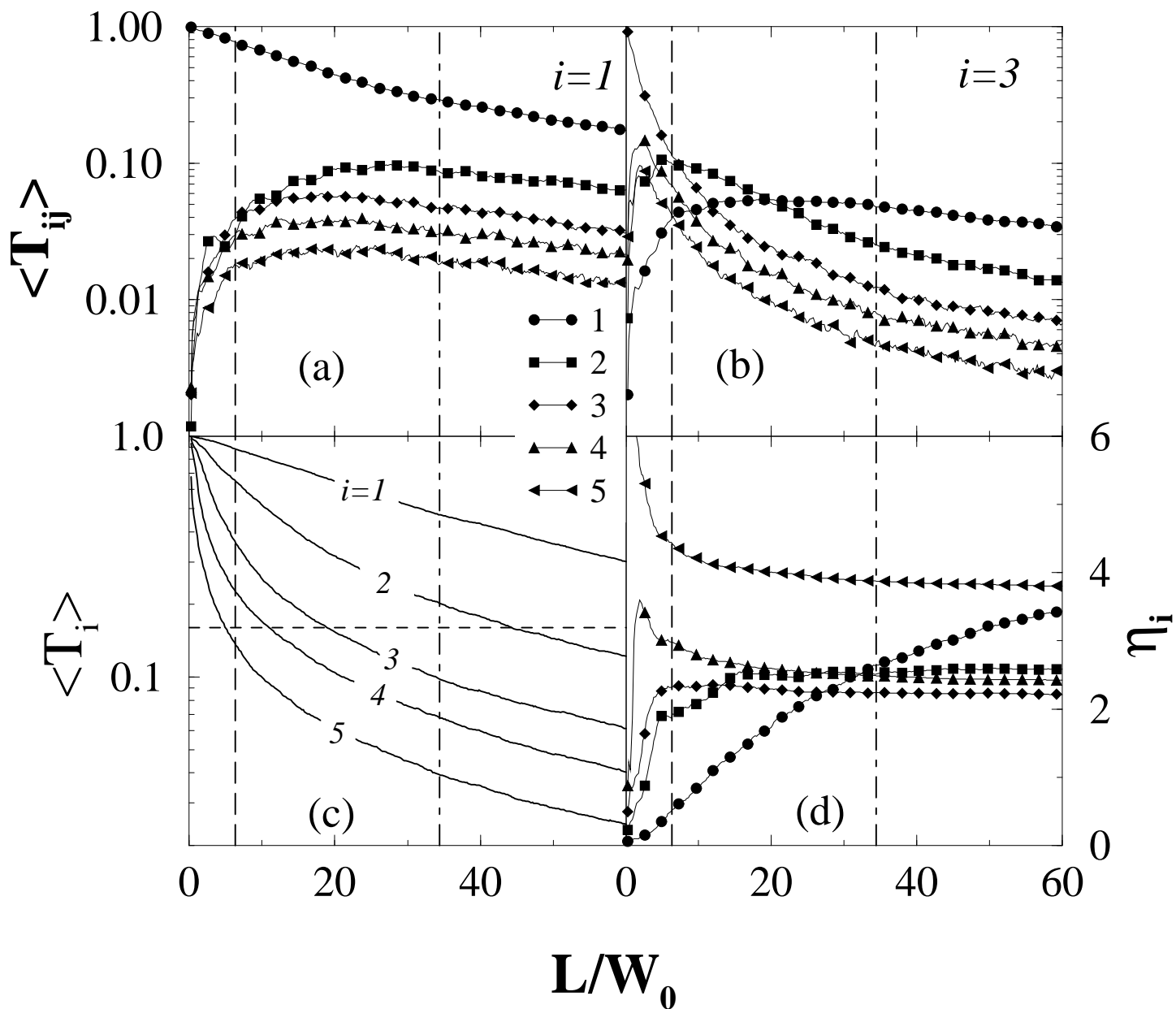
FIG. 2. (a) Averaged transmission coefficients $\langle T_{ij} \rangle$ versus L/W_0 (incoming mode $i = 1$, outgoing mode j). (b) The same as (a) for $i=3$. (c) Averaged transmission coefficients $\langle T_i \rangle$ versus L/W_0 . At $\langle T_i \rangle = 0.16$ (horizontal dashed line) incoming modes $i = 3, 4, 5$ have the same probability densities as shown in the inset of Fig. 3. (d) Enhanced backscattering factor η_i versus of L/W_0 . Vertical long-dashed and dotted-dashed lines are drawn at $L = \ell$ and $L = \xi$ respectively.

FIG. 3. (a) Distribution of $x = T_i/\langle T_i \rangle$ for different values of $\langle T_i \rangle$. The inset shows the distribution for $i = 3, 4, 5$ having the same average $\langle T_i \rangle \approx 0.16$ (see Fig. 2c). The smoothed curves are superimposed to the histograms to guide the eye. (b) Distribution of $x = T_{ij}/\langle T_{ij} \rangle$ for different lengths L/ξ . The straight line corresponds to the exponential distribution.

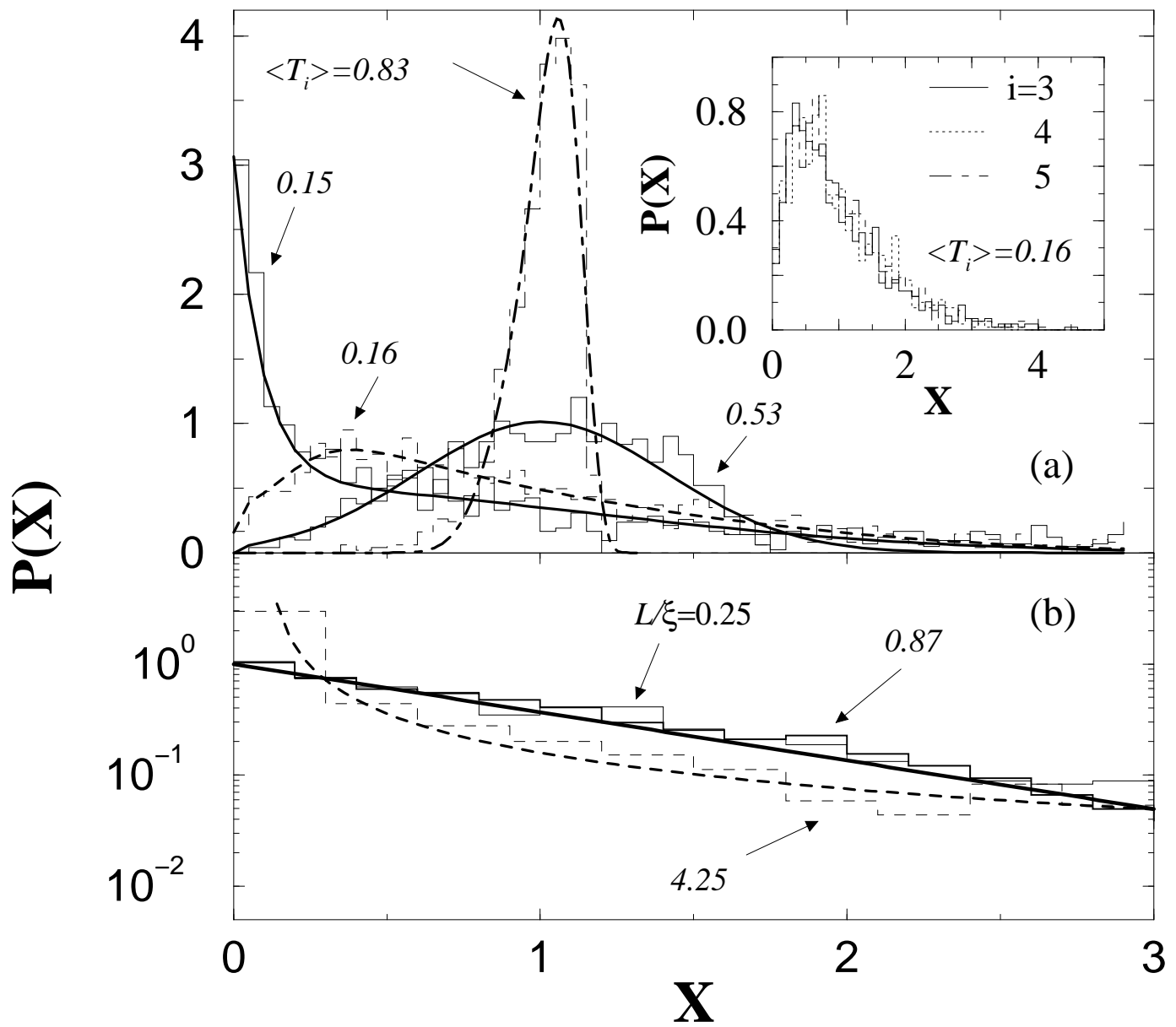
FIG. 4. Distribution of $\ln(\tau)$ with $\tau = T_i, T_{ij}$ for different values of $\langle \ln(\tau) \rangle$. The inset shows the distribution of the conductance G for two different lengths of the disordered region. Continuous lines are fittings to lognormal distributions having $\sigma_{\langle x \rangle}^2 = 3/2\langle x \rangle$, for $x = \ln(\tau)$, and $\sigma_{\langle x \rangle}^2 = 2\langle x \rangle$ for $x = \ln(G)$.



A. Garcia-Martin et al.
 Fig. 1 (PRL)



A. Garcia-Martin et al.
 Fig. 2
 (PRL)



A. Garcia–Martin et al.
 Fig. 3
 (PRL)

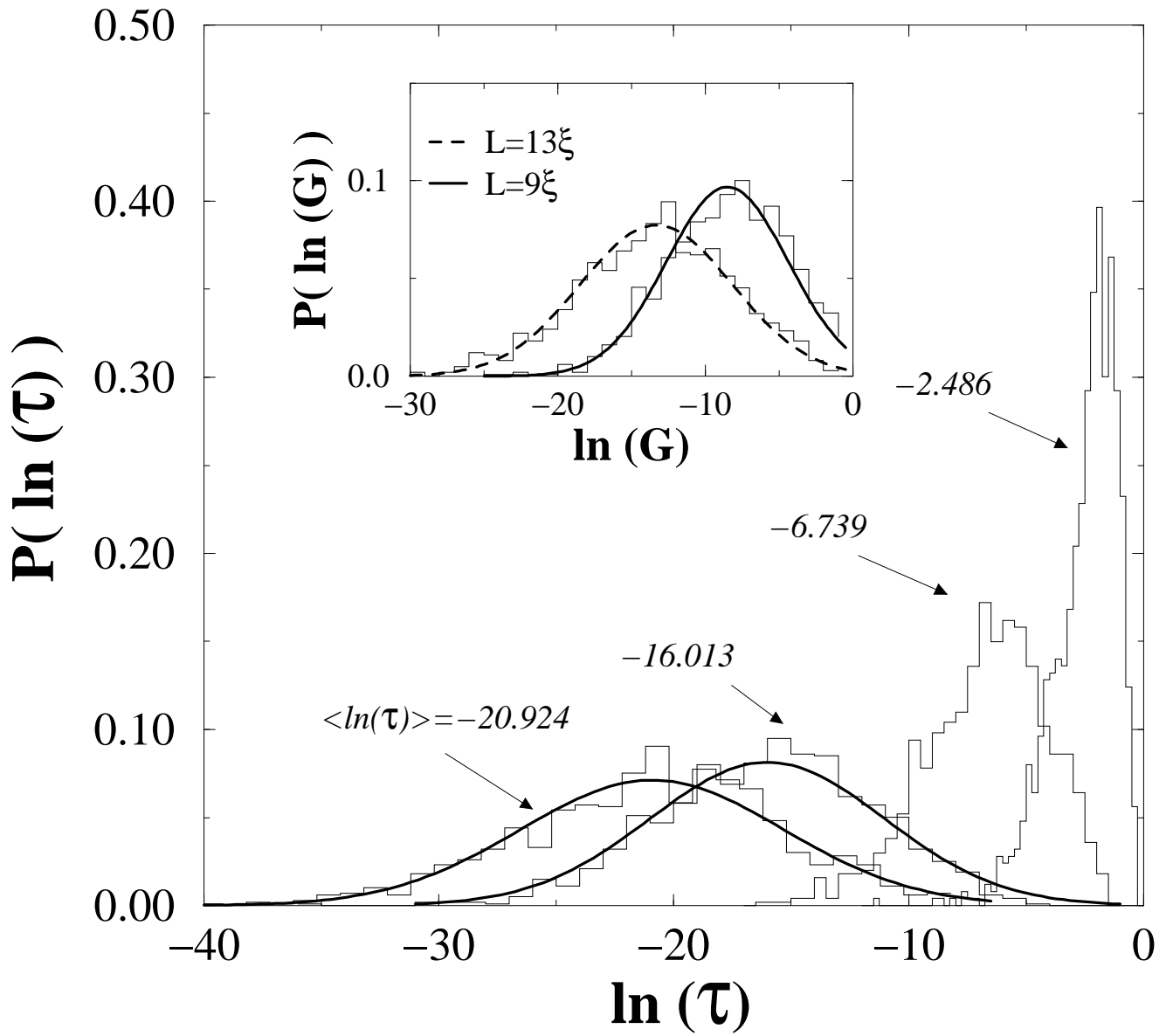


Fig. 4
A. Garcia-Martin et al.
(PRL)